Journal of Asian Earth Sciences 180 (2019) 103869

Contents lists available at ScienceDirect

Journal of Asian Earth Sciences

journal homepage: www.elsevier.com/locate/jseaes

Full length article

Coulomb stress perturbation after great earthquakes in the Sumatran subduction zone: Potential impacts in the surrounding region

Qiang Qiu[a,b], Chung-Han Chan[b,*]

[a] Asian School of the Environment, Nanyang Technological University, Singapore
[b] Earth Observatory of Singapore, Nanyang Technological University, Singapore

ARTICLE INFO

Keywords:
Coulomb stress
Sumatra
Postseismic relaxation
Mentawai seismic gap
Volcano
Tsunami

ABSTRACT

The Sumatran subduction zone has been seismically very active compared with other major subduction zones in the world. Since 2004, a sequence of large earthquakes ruptured along the trench, including the 2004 M_w 9.2 Sumatra-Andaman, the 2005 M_w 8.6 Nias-Simeulue, the 2007 M_w 8.4 Bengkulu, the 2010 M_w 7.8 Mentawai tsunami earthquakes and numerous moderate and small events. These earthquakes released stress over tens of seconds to minutes, disturbing the lithosphere and asthenosphere across a broad region. As earthquake-introduced stress disturbance can trigger tremendous aftershocks and sometimes precipitate large earthquakes in their vicinity, gaining a detailed picture of spatial and temporal stress evolution on the fault and its neighboring faults is crucial for seismic forecasting. Here, we have developed spatiotemporal Coulomb stress models for the Sumatran region, which includes the Sumatran subduction zone and the Sumatran fault, using a well-studied postseismic model. This postseismic model is constrained by decade-long time series of geodetic observations from the Sumatran GPS Array (SuGAr) and from tide gauge data in Southeast Asia. We show that Coulomb stress changes imparted by co- and post-seismic processes of previous great ruptures could well explain the temporal and spatial connection between seismicity and stress evolution. Most importantly, our results reveal that the stress in the Mentawai seismic gap of the Sumatran subduction zone was loaded by more than two bars. These stress perturbations could potentially trigger the rupture of the Mentawai seismic gap, which was already overdue in the last seismic cycle. Now, the likelihood for the failure of this gap is even higher than before 2004. We also find that along the Sumatran fault stress has increased to more than one bar, which may explain the surrounding seismicity. Consequently, we highlight the considerable seismic hazard and associated tsunami threat to the neighboring regions.

1. Introduction

The world's largest earthquakes occur along the converging plate boundaries in subduction zones by rupturing large patches of megathrusts. These giant earthquakes release accumulated stress on the faults within seconds to minutes, disturbing the stress state of the lithosphere and asthenosphere system (Ammon et al., 2005; Banerjee et al., 2007; Chlieh et al., 2007; Hughes et al., 2010; Wiseman et al., 2015). The stress disturbances from these earthquake ruptures can drive pore pressure migrations that further trigger large earthquakes (Hughes et al., 2010), and push weak portions of faults that continued to slip, so called afterslip (Barbot et al., 2009; Hsu et al., 2002; Johnson et al., 2006; Perfettini and Avouac, 2007), and also accelerate viscoelastic flow in the upper mantle (Broerse et al., 2015; Freed et al., 2006; Hoechner et al., 2011; Hu et al., 2016; Hu and Wang, 2012; Moore et al., 2017; Panet et al., 2010; Pollitz et al., 2006; Suito and Freymueller, 2009; Sun et al., 2014; Wiseman et al., 2015). Transient postseismic processes of the afterslip and viscoelastic flow are capable of introducing stress loading on neighboring faults or sometimes on distant faults, causing them closer to fail (Bürgmann et al., 2002; Felzer et al., 2002; Freed and Lin, 2001; Hearn et al., 2002). Occasionally, the postseismic relaxation could lead the shallow part of the megathrust to rupture as a tsunamigenic earthquake (Tsang et al., 2016). The transient processes can last for months, years, decades (Copley, 2014; Suito and Freymueller, 2009), or even longer (Wang et al., 2012). Consequently, precisely investigating the spatiotemporal stress evolution within subduction zones is fundamental for comprehensive seismic and tsunami hazard assessments.

Such assessment is crucial for the Sumatran subduction zone. Various portions of the Sumatran megathrust ruptured during the 2004

* Corresponding author.
E-mail address: hantijun@googlemail.com (C.-H. Chan).

https://doi.org/10.1016/j.jseaes.2019.103869
Received 9 November 2018; Received in revised form 14 May 2019; Accepted 24 May 2019
Available online 25 May 2019

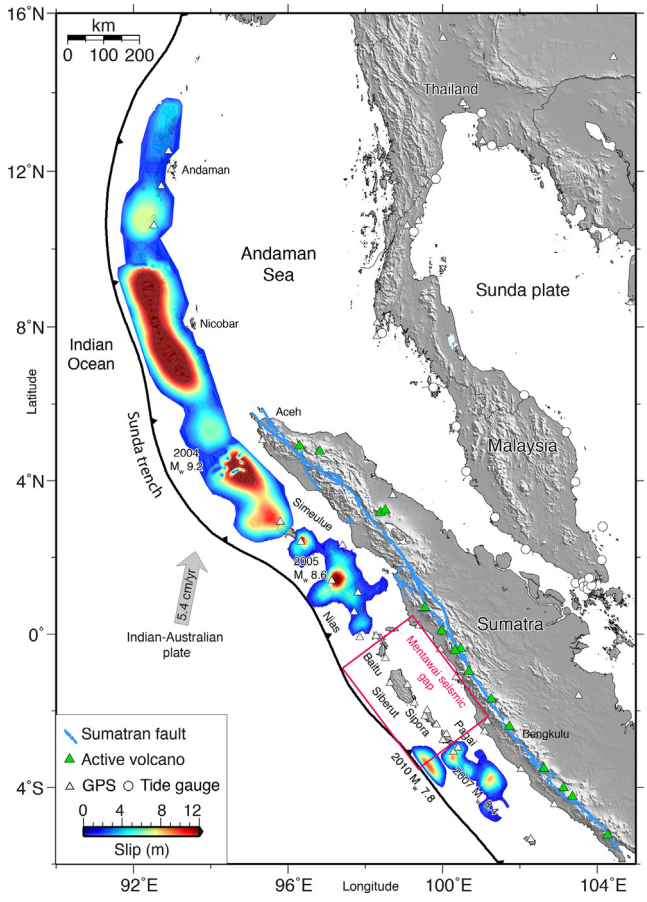

Fig. 1. Published slip models of the great earthquakes in the Sumatran subduction zone since 2004. The colored areas represent slip models of the great earthquakes. Geographically from north to south, they are the 2004 M_w 9.2 Sumatra-Andaman (Chlieh et al., 2007), the 2005 M_w 8.6 Nias-Simeulue (Konca et al., 2007), the 2007 M_w 8.4 Bengkulu earthquakes (Konca et al., 2008) and the 2010 M_w 7.8 Mentawai tsunami earthquake (Hill et al., 2012). The colorbar is saturated at 12 m. The red rectangle delineates the so-called Mentawai seismic gap. The green triangles show the locations of active volcanoes on the Sumatran mainland. The blue alignments show the Sumatran fault. (For interpretation of the references to color in this figure legend, the reader is referred to the web version of this article.)

M_w 9.2 Sumatra-Andaman (Ammon et al., 2005; Chlieh et al., 2007), the 2005 M_w 8.6 Nias-Simeulue (Kreemer et al., 2006; Hsu et al., 2002; Konca et al., 2007), the 2007 M_w 8.4 Bengkulu (Konca et al., 2008), and the 2010 M_w 7.8 events (Hill et al., 2012) (Fig. 1). These ruptures left a large segment of the trench, the Mentawai gap, unbroken, with the patch poised for a potential $M_w \geq 8.8$ event (MUHARI et al., 2010; Natawidjaja, 2009). Furthermore, coral microatoll measurements in this gap indicate a super-cycle earthquake recurrence of ca. 200 years (Sieh et al., 2008), and with the last great earthquake there in 1797 (Natawidjaja et al., 2006), the next rupture is expected in the coming decades (Sieh et al., 2008). Assessing the gap's stress status is critical, as any stress perturbation might trigger its rupture, resulting in ground shaking and tsunami aimed directly at the highly populated cities of Padang and Painan in Sumatra (Li et al., 2012; MUHARI et al., 2010).

Additionally the 1900 km-long Sumatran fault (Sieh and Natawidjaja, 2000) on the mainland is close to these great earthquake rupture regions, and 13 active volcanoes are in its vicinity (Fig. 1). Co- and post-seismic stress perturbations from these megathrust earthquakes may have stressed the Sumatran fault and these volcanoes, and could bring failures of the fault in advance and could trigger volcano activities.

In this paper, we implement the well-studied coseismic slip models for the above-mentioned great earthquakes and the associated postseismic deformation models to evaluate the spatiotemporal stress evolution in the Sumatran subduction zone, on the Sumatran fault, and under the active volcanoes, respectively. We find that previous earthquakes elevated the stress level in the Mentawai gap. Stress in most segments of the Sumatran fault increased, except for the segment close to the Mentawai gap, where the stress level was elevated only moderately. Under the 13 active volcanoes, the coseismic ruptures reduced pressure by more than 0.2 bar, while the postseismic processes have affected the pressure moderately. However, the interaction between the Sumatran fault and these active volcanoes needs to be recognized. In summary, as the stress changes in the Mentawai gap and on the Sumatran fault are high (> 1 bar), we suggest that seismic and the associated tsunami hazards in this region have significantly increased, which should be reflected in hazard assessment and mitigation programs.

2. Methodology

2.1. Geodetic data and postseismic models

Indonesia is called an "Island country" as it is composed of thousands of islands varying in size. Some of these islands are directly above the plate boundary between the subducting Indo-Australian and Sunda plates, forming megathrusts in the Java and Sumatran subduction regions. In the Sumatran subduction zone, a chain of islands located directly above the seismogenic region provides a unique opportunity to deploy equipment to capture motion of the megathrust and in the mantle, down to tens to hundreds of kilometers into the earth's subsurface. The Sumatran GPS Array (SuGAr) is deployed on this island chain and on the Sumatran mainland, monitoring surface deformation on a millimeter scale (Feng et al., 2015). The SuGAr network, which has been monitoring the Sumatran subduction zone since 2002, has recorded deformations caused by detectable tremendous small earthquakes, great earthquakes and giant earthquakes (Feng et al., 2015). The extensive dataset contains complex information from multiple earthquakes, and has afforded detailed interrogation of the movements of the megathrust, for example, coseismic slip processes (Hill et al., 2015, 2012; Konca et al., 2007, 2008; Salman et al., 2017) and postseismic relaxation following earthquakes (Feng et al., 2016; Hsu et al., 2002; Hu et al., 2016; Kreemer et al., 2006; Masuti et al., 2016; Qiu et al., 2018; Salman et al., 2017; Tsang et al., 2016; Wiseman et al., 2015).

The GPS measurements show the ground surface moved rapidly in the early stages of postseismic relaxation following megathrust earthquakes, before slowing down to progressively longer time periods (Feng et al., 2015). These transient motions may reflect the likely movements on the megathrust, on the neighboring fault systems, and in the upper mantle. Qiu et al. (2018) combined these GPS time series together with far-field tide gauges in Malaysia and Thailand to interrogate these transient motions on the fault and in the continental mantle wedge from early 2005 to 2014. They modeled the transient motions on the fault as afterslip processes and in the mantle wedge as viscoelastic flows, using a Kalman-filter-based joint inversion approach. The technique inverts a kinematic process of the slip and viscous strain (Barbot et al., 2017) in the mantle wedge without a prior assumption on the possible rheology model.

Qiu et al. (2018) have shown that the afterslip on the megathrust following great earthquakes is primarily located in the periphery of their coseismic slip patches, and the viscoelastic flows are mainly distributed deep, down-dip of the coseismic slip region in the mantle wedge (Fig. 2). They show spatiotemporal modifications in the ca. 9 years' modeling time period. The spatial and temporal dependencies of the afterslip and viscoelastic flow may have modulated the stress fields by stress loading of existing faults, redistributing the stress along the megathrust itself and its surrounding tectonic structures. Thus, we

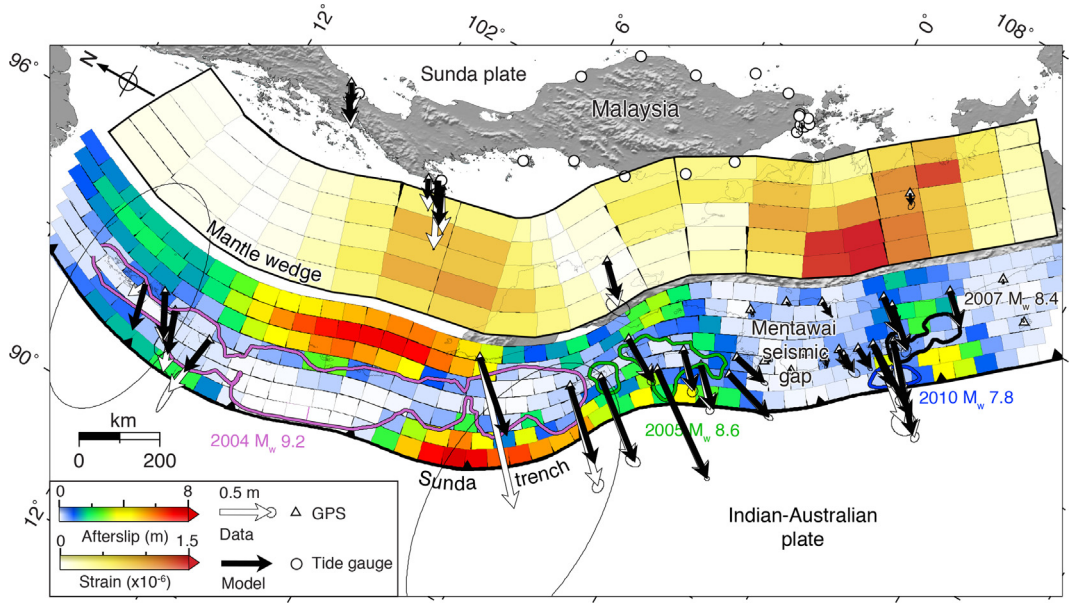

Fig. 2. Cumulative afterslip on the megathrust and viscous strain in the mantle wedge estimated from early 2005 to 2014 (modified from Qiu et al. 2018). The colors of the mantle wedge present the second invariant strain tensor with color saturated at 1.5×10^{-6}. The color on the fault patches shows the afterslip estimated and saturated at 8 m. Both near-field GPS and far-field tide gauges were used for postseismic modeling. The colored contours represent the same earthquake ruptures as in Fig. 1.

use this well-estimated afterslip and viscous strain variations to evaluate the spatiotemporal stress changes on fault systems, including the Sumatran subduction zone and the Sumatran fault, and to examine pressure changes under the active volcanoes in Sumatra.

2.2. Coulomb stress

Coulomb stress model is a physics-based model and a powerful tool for earthquake forecasting (e.g., Chan et al. 2010; Catalli and Chan, 2012). For example, spatial distribution of aftershocks and earthquake interactions have been successfully modeled as a response of Coulomb stress change induced by previous neighboring earthquakes (Catalli and Chan, 2012; Chan and Stein, 2009; Harris, 1998; King and Cocco, 2001). Here we use the COULOMB 3.4 code (Toda et al., 2011) to calculate the stress changes from the estimated slip and viscous strain in homogenous media (Qiu et al., 2018). Since this stress model is physics-based, the stress calculations are based on numerous a priori assumptions, such as, target depth of calculation and receiver fault planes. Such information, however, is usually unclear, resulting in large uncertainties in calculations, which in turn bias interpretation of earthquake triggering and forecasting. Previous studies suggested that spatial variation receiver faults that match the neighboring focal mechanism can largely reduce the uncertainty and explain the seismicity pattern (e.g., Chan et al., 2010; Toda et al., 2008). Further, Catalli and Chan (2012) conclude that target depth plays a fundamental role in stress calculation, and by selecting the maximum stress over the entire seismogenic depth, can sufficiently explain seismicity pattern regardless of different tectonic regimes.

In this study, we implemented the approach by Catalli and Chan (2012) to evaluate Coulomb stress in the Sumatran subduction zone. Basically this approach discretizes the study area into layered computational grids at various depths. At each grid, the receive fault is assumed to be the nearest reference focal mechanism. Finally the maximum Coulomb stress change over the entire computational depth range at each grid will be used for further interpretation. In Sumatra we defined the computational domain ranging from 90°E to 105°E, from 6°S to 16°N on a 0.2-degree horizontal grid, and 20-km depth grid interval. We tested different friction coefficients and obtained undistinguishable results; thus we fixed the friction coefficient at 0.4 for all calculations. At each grid point, we searched for the closest focal mechanism solution from gCMT (https://www.globalcmt.org/CMTsearch.html) to determine a receiver fault plane for each calculation grid. We evaluated the stress at a 10-km depth with a right-lateral motion for the Sumatran fault, and we calculated the pressure changes at the depth of 10 km at the locations of the 13 active volcanoes on the Sumatran mainland (Fig. 1).

3. Results

3.1. Coseismic stress change

When calculating the coseismic stress change for each megathrust earthquake in the Sumatran subduction zone, we chose the coseismic slip models, which incorporated as many available observations (e.g., GPS data, seismicity, tide data) as possible. These models included Chlieh et al.'s (2007), Konca et al.'s (2007), Konca et al.'s (2008) and Hill et al.'s (2012) for the 2004 M_w 9.2 Sumatra-Andaman, the 2005 Nias-Simeulue, and the 2010 M_w 7.8 Mentawai tsunami earthquakes, respectively (Fig. 1). We show the maximum stress at each grid over the entire 100 km seismogenic depth in Fig. 3 and aftershocks from the ISC catalog spanning from 2004 to 2014. In general, the maximum stress changes are positive almost everywhere along the entire subduction zone, with only a few patches where stress decreased. These places are, for example, a small portion of the Mentawai earthquake rupture region west of the Pagai Island, down-dip of the Bengkulu slip area, and spotted patches downdip of the Sumatra-Andaman rupture. Overall these stress-reduced regions are small and with low seismic activity, while almost all the seismicity occurred within areas of increased stress, suggesting Coulomb stress changes enable good spatial forecasting of seismicity in this region.

These great earthquakes increased stress over a broad region, reaching ca. 1000 km to Malaysia and Thailand and across the whole Sumatran mainland (Fig. 3). In addition, we notice another intriguing feature of the correlation between the increased stress and the increased out-rise seismicity between 6°N to 8°N. The significant stress increase in this region further suggest that the coseismic slip may have reached the trench and triggered these aftershocks (Sladen and Trevisan, 2018).

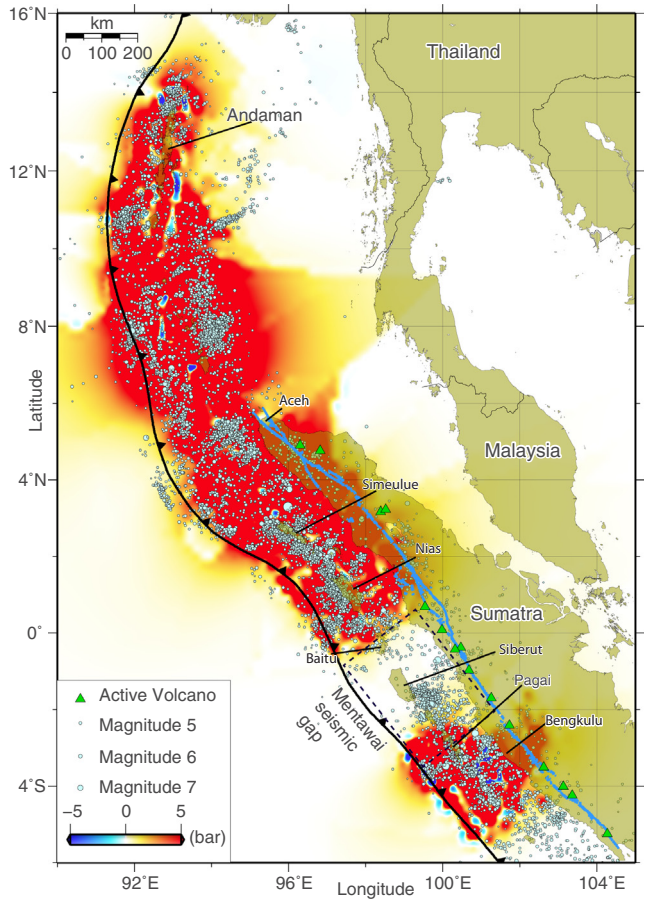

Fig. 3. A Coulomb stress model from the coseismic slip models of the great earthquakes shown in Fig. 1. The color represents the maximum stress changes over 100 km depths at each grid, with a scale saturated at 5 bars. The white circles indicate seismicity from 2004 to 2014 from the ANSS catalog.

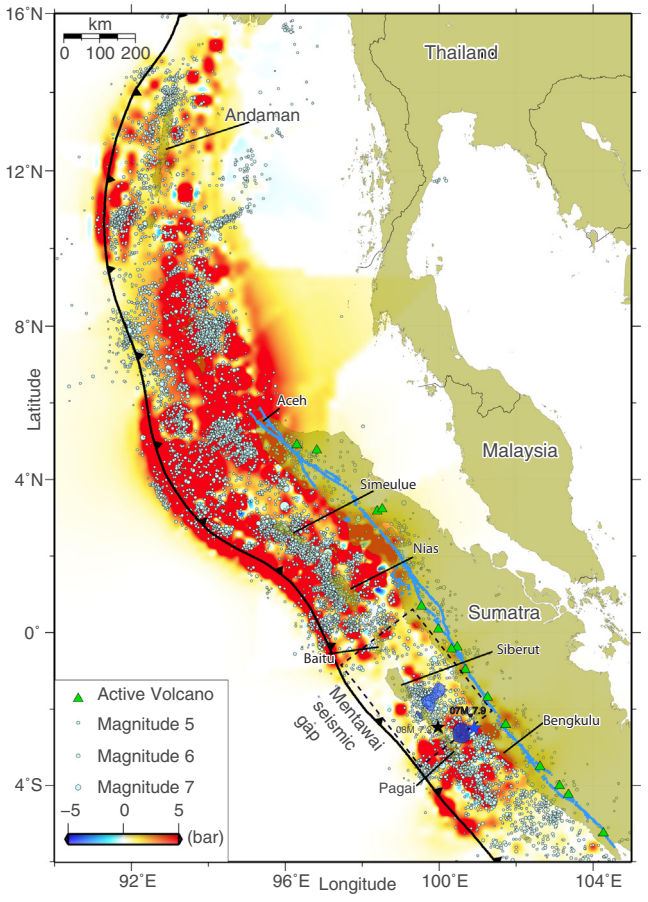

Fig. 4. A Coulomb stress model from the postseismic deformation study of Qiu et al. (2018). It is identical to the model in Fig. 3, but it shows the cumulative postseismic stresses from early 2005 to 2014. The blue star indicates the hypocenter of the 2007 M_w 7.9 earthquake with blue region showing the estimated rupture region (Konca et al., 2007). The black star presents the hypocenter of the 2008 M_w 7.2 Mentawai earthquake (Salman et al., 2017). The color represents the maximum stress changes over 100 km depths at each grid, with a scale saturated at 5 bars. (For interpretation of the references to color in this figure legend, the reader is referred to the web version of this article.)

The 2004, 2005, 2007, and 2010 earthquakes stressed the northern part of the Sumatran fault from Aceh all the way to Baitu Islands and the Bengkulu segment of the Sumatran fault in the south (Fig. 3). In the middle segment, close to the Mentawai seismic gap region, the stress was moderately raised (< 1 bar), while the stresses at the boundaries of Baitu Island to the north and especially at the boundary (the region outlined by the dashed rectangular) to the south were elevated (> 5 bars).

3.2. Postseismic stress evolution

The stress evolution during postseismic period were evaluated by the well-estimated afterslip on the megathrust and the viscoelastic flows in the mantle wedge by Qiu et al. (2018) for the same area as the coseismic stress calculations (shown in Fig. 3). Similarly to coseismic stress modeling, we show the maximum cumulative stress (from early 2005 to 2014) at each grid over the seismogenic depth (Fig. 4). Similarly to the coseismic stress changes, postseismic stress evolution, in general, explains well the spatial pattern of the aftershocks (Fig. 4). In some locations, the postseismic stress pattern is better correlated with the aftershocks than that of coseismic stress changes (e.g., increased out-rise aftershocks offshore of the Andaman Islands between 10°N to 15°N, offshore of Aceh between 2°N-6°N, or offshore of Nias between 1°N to 2°N). The deep afterslip following these great earthquakes further enhanced the stress level at the Sumatran fault in the Aceh and Nias segments. The Sumatran fault in the Bengkulu region was also elevated by postseismic relaxation following the 2007 earthquake.

In the Mentawai seismic gap region, the stress modulations during the postseismic period were more complex than the coseismic stress changes. The stress level in Baitu Island region was highly elevated and reached further south than the coseismic process due to afterslip on the megathrust (Fig. 2). Downdip of north Pagai Island, the stresses were enhanced by the downdip of the afterslip following the 2007 Bengkulu earthquake (Fig. 3). Interestingly, stress increased on two isolated patches northeast and south of Siberut Island. The northeast patch was related to the afterslip process on the megathrust fault as the stress response to the M_w 7.9 aftershock following the 2007 M_w 8.4 Bengkulu mainshock (Konca et al., 2007; Tsang et al., 2016). The southern patch was connected with the continued slip on the fault following the 2008 M_w 7.2 earthquake (Salman et al., 2017). We also obtained moderate stress increase on the Sumatran fault in the seismic gap.

3.3. Spatiotemporal postseismic stress changes on the Sumatran fault

We calculated the postseismic stress evolution on the Sumatran fault with right-lateral motion. We first tested stress calculations from 10 to 30 km depths, and concluded that there was no significant variation across this depth range (Fig. S1). Thus we present the postseismic stress evolution and also the coseismic stress changes on the Sumatran fault at the depth of 10 km (shown in Fig. 5). In addition, we plot aftershocks (from the ISC and ANSS catalogs) within a 15-km range surrounding the

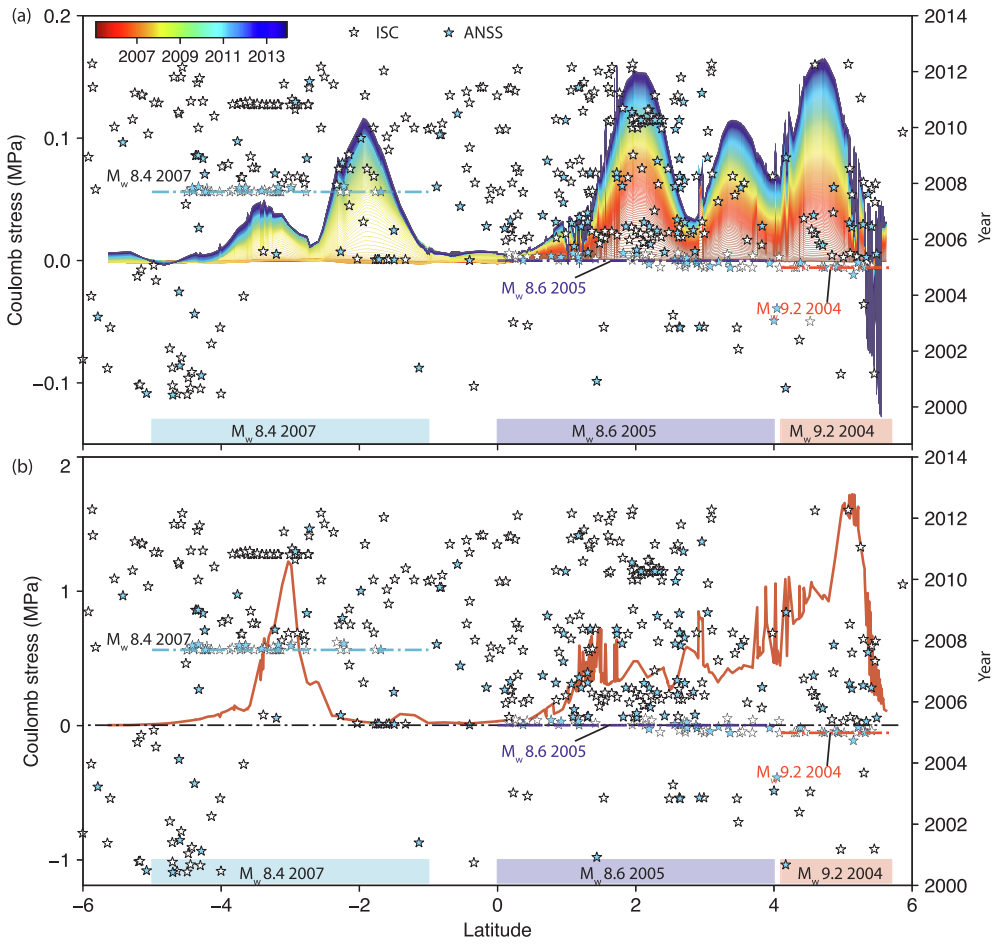

Fig. 5. A Coulomb stress model for the Sumatran fault for (a) Postseismic stress evolution and (b) Coseismic stress changes. The stress was calculated at a 10-km depth with a right-lateral receiver slip direction. The white and light-blue stars show seismicity from the ISC and ANSS catalogs, respectively, with a time period spanning from 2000 to 2014. The red, blue and cyan dashed lines indicate the times of the 2004, 2005, and 2007 earthquakes, respectively. The warm and blue colors show the spatiotemporal evolution of postseismic stress. (For interpretation of the references to color in this figure legend, the reader is referred to the web version of this article.)

Sumatran fault, shallower than the depth of 60 km, in Fig. 5. We notice that the seismicity rate after the 2004 Sumatra-Andaman earthquake is much higher in the southern part of the 2004 rupture between ca. 6°N to 4°N, and spatially extending further south from ca. 2°N to 4°N in the region with the 2005 rupture. The raised seismicity gradually subsided as the stress rate decayed, but the spatiotemporal changes are well correlated with the stress evolution in the 2004 rupture segment following the earthquake.

Further south of the Sumatran fault, near the 2005 Nias rupture, we have found a similar highly elevated seismicity rate following the earthquake (Fig. 5). During the coseismic period, the spatial distribution of the subsequent seismicity is highly correlated with the largest area of elevated stress (e.g., around 2.0°N and 3.5°N). These seismicity numbers are positively correlated with the cumulative postseismic stress. We notice two stress-concentration regions in the 2005 Nias rupture area, with the southern one (between 0° and 3°N) gaining more stress than the northern one (3°N to 4°N) due to the larger transient slip on the megathrust (Fig. 2). We obtain high dense distributed seismicity in the southern segment compared to the northern segment, indicating that the transient motions on the fault and the mantle flow may have promoted the failures of these earthquakes. These transient motions are still ongoing (Qiu et al., 2018), inferring its continuously impact on seismicity activity.

Moving towards the southern segment of the Sumatran fault near the 2007 Bengkulu rupture patch (from 5°S to 1°S), the seismicity rate before 2004 was low (Fig. 5), especially in the northern part (from 1°S to 3°S), where seismicity was almost absent, while seismicity rate in the southern part (from 5°S to 3°S) was moderate. Similarly, after the Bengkulu rupture, the seismicity rate immediately jumped above the background rate, and continued to rise following the earthquake. More intriguing is the finding that seismicity density in the southern part is much higher than that of the northern part immediately after the earthquake, suggesting that the southern part may be highly stressed and closer to failure, and then triggered by the large stress loading from the coseismic release.

In between 1°S and 1°N, within the Sumatran fault segment near the Mentawai seismic gap, we observe almost no earthquakes from 2000 to 2005. However, after the Nias and Bengkulu earthquakes, the seismicity rate continued rising over time (Fig. 5), implying that the co- and postseismic stresses may have loaded this portion of the Sumatran fault.

3.4. Pressure evolution of active volcanoes on the Sumatra Island

We calculated the time evolution of pressure changes at the depth of 10 km for the 13 active volcanoes (green triangles in Fig. 1) on the Sumatran mainland based on the estimated afterslip and viscous strain. We also calculated the pressure changes under these volcanoes from the coseismic ruptures. The pressure changes from co- and post-seismic processes are shown in Fig. 6.

The coseismic ruptures depressed all the 13 volcanoes, i.e. in the 2004 rupture region, the pressure reduction reached a maximum of ca. 0.3 MPa, and the seismicity within 15 km of the volcanoes increased for several months immediately following the earthquake, and then disappeared. The sudden seismicity quiescence might be associated with the pressure increase from postseismic processes. A similar phenomenon occurred under the volcanoes near the 2005 rupture region (Figs. 1 and 6). While in the 2007 Bengkulu rupture region, no seismicity was associated with the pressure decrease following the coseismic rupture. The absence of seismicity in the vicinity of these volcanoes might have been caused by a lower maximum pressure decrease

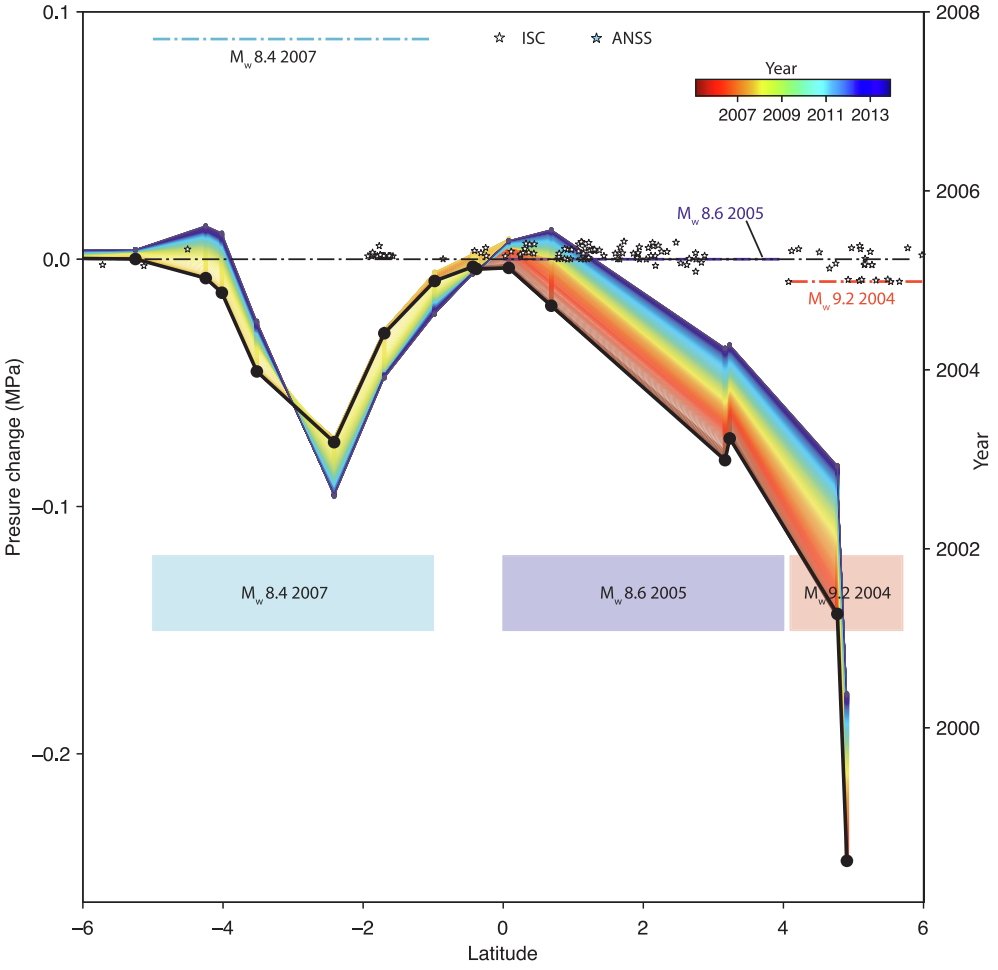

Fig. 6. Coseismic and postseismic pressure changes calculated at 10 km deep for the 13 active volcanoes on the Sumatran mainland. The colorbar indicates pressure changes with time, with the black thick line showing coseismic pressure changes. The locations of the active volcanoes are shown in Fig. 1. The white and light-blue stars show the seismicity from the ISC and ANSS catalogs, respectively, with a time period spanning from 2000 to 2014. The red, blue and cyan dashed lines indicate the times of the 2004, 2005, and 2007 earthquakes, respectively. (For interpretation of the references to color in this figure legend, the reader is referred to the web version of this article.)

than in the cases of the 2005 Nias-Simeulue and the 2004 Sumatra-Andaman earthquakes. The total pressure changes in the Bengkulu segment vary from north to south: Between 0° to 3°S, the pressure is declining, which may facilitate further dilatation effects and/or promote seismic activities; from 6°S to 3°S, pressure under the active volcanoes is building up following the 2007 earthquake, which may suppress possible dilatation in the following years.

4. Discussion

Our co- and post-seismic stress models have explained the evolution of seismic activities in the Sumatran subduction system remarkably well, indicating that Coulomb stress modeling by using the spatially variable receiver slip direction from neighboring focal mechanism and presenting the maximum stress changes over the entire seismogenic depth can robustly assess the earthquake triggering and fault interaction (Catalli and Chan, 2012; Chan et al., 2010; Chan and Stein, 2009). While a sufficient number of GPS stations in the Mentawai gap and further south until Pagai Islands (Fig. 1) provide good constrains for our stress calculations, some uncertainties may remain, mostly due to resolution limits in the measurements-driven geodetic slip inversions. Firstly there are multiple postseismic mechanisms and their resulting natural trade-offs; secondly, the afterslip process mostly occurred updip and down-dip of the coseismic slip on the megathrust (e.g., Hsu et al., 2002; Kreemer et al., 2006; Qiu et al., 2018; Tsang et al., 2016), where geodetic observations are rare. To resolve these uncertainties, future large-scale measurements in the ocean and on land are highly recommended. In comparison to the post-seismic slip uncertainties, the coseismic slip is well constrained as the ruptures occurred beneath the fore-arc islands chain and a wealth of data is available; thus the associated coseismic stress changes are well determined.

The Mentawai segment of the Sumatran subduction zone ruptured historically in 1797 and 1833 in $M_w > 8.5$ events (Natawidjaja et al., 2006) (Fig. 7). No single earthquake with $M_w > 8$ has occurred since then, but coral data in this region indicate an earthquake super-cycle with a return period of ca. 200 years (Sieh et al., 2008). In addition, modeling based on coral measurements and geodetic data and long-term GPS measurements shows that this portion of the megathrust has been highly coupled throughout at least the past half-century, indicating that stress has been accumulating since 1797 and 1883 (Chlieh et al., 2008; Natawidjaja et al., 2007), corresponding to a slip deficit of ca. 10 m, if we assume a slip deficit rate of 45 mm/year (Linette et al., 2010; Natawidjaja et al., 2006). The Mentawai seismic gap is thus overdue, and possible stress disturbances from neighboring ruptures will likely push the segment to failure. Postseismic stress loading by 1–2 bars has been proposed to be responsible for triggering great earthquakes on distant faults. Examples include delayed triggering of the 1999 M_w 7.1 Hector Mine event by the 1992 M_w 7.3 Landers earthquake in southern California (Freed and Lin, 2001) and the 1999 M_w 7.1 Düzce event by the M_w 7.5 Izmit earthquake in Turkey (Hearn et al., 2002). Our coseismic and especially postseismic stress models loaded this seismic gap with the maximum stress of more than 5 bars, providing a mature stress condition for nucleating earthquakes (Dieterich, 1992; Duan and Oglesby, 2006; Lapusta and Rice, 2003). Additionally, our stress model for the 2008 M_w 7.2 rupture (Fig. 7) further loaded the Mentawai gap, which increased stress between Sipora and Pagai Islands by more than 2 bars. The spatial stress pattern in the Mentawai gap is thus indicating a critical state. The potential rupture will not only cause

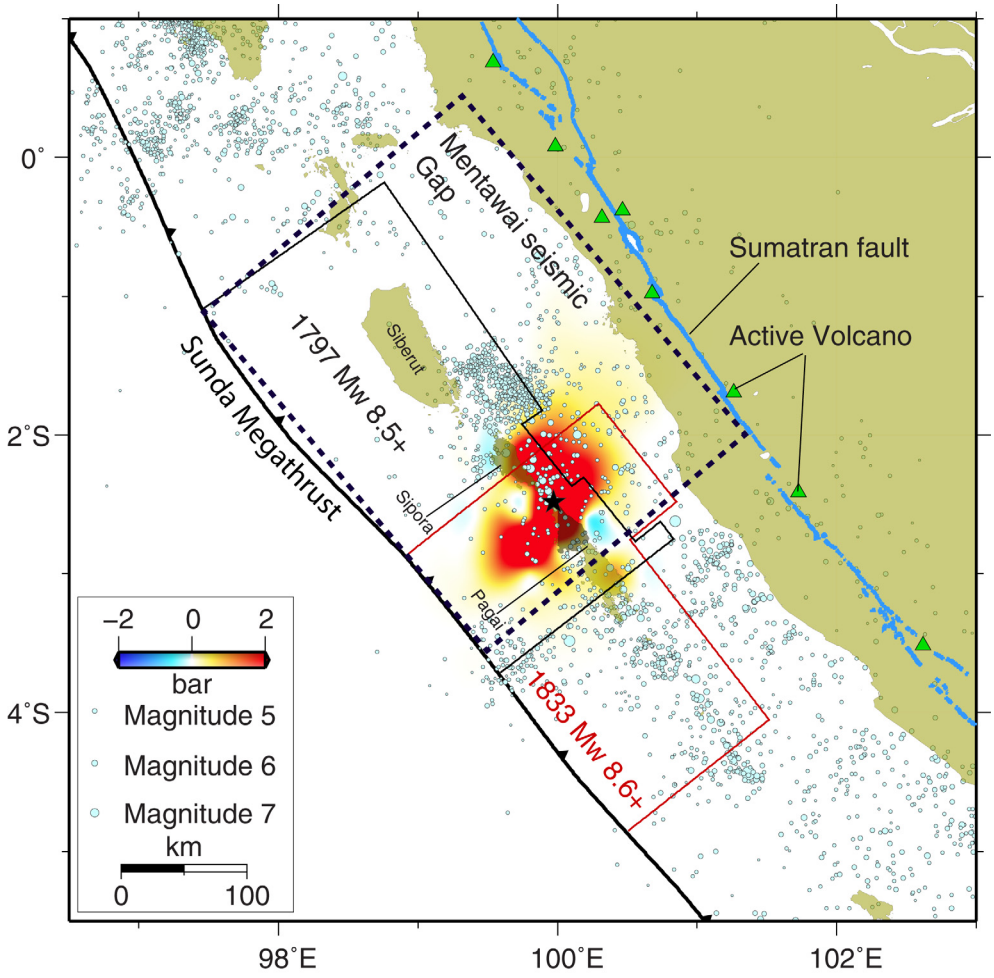

Fig. 7. Co- and post-seismic Coulomb stress changes from the 2008 M_w 7.2 Mentawai earthquake (Salman et al., 2017). The black star marks the epicenter of the earthquake. The black and red thin geometries show the 1797 and 1833 rupture patches (Natawidjaja et al., 2006), respectively. The black dashed line represents the remaining Mentawai seismic gap. The warm and blue colors show the total stress from coseismic stress and 5.6 years of postseismic relaxation period. (For interpretation of the references to color in this figure legend, the reader is referred to the web version of this article.)

strong ground shaking on the Mentawai islands (e.g., Siberut, Sipora and Pagai), but also trigger a 5–6 m' tsunami that will arrive at the highly populated cities (e.g., Padang, Painan) and the coastal area in the west Sumatra within ca. 30 min (Borrero et al., 2006; Li et al., 2012; MUHARI et al., 2010).

In addition, large earthquakes may affect activities of nearby volcanoes. For example, in the Chile subduction zone, pore fluid was driven by the 2010 M_w 8.8 Maule megathrust earthquake, triggering subsidence surrounding the fore-arc volcanoes (Pritchard et al., 2013), and also viscoelastic flow below this volcanic chain (Klein et al., 2016; Li et al., 2018). Similarly, the Mentawai gap is forecast to rupture in $M_w \geq 8.8$, which will likely affect that the neighboring volcanoes.

We have found elevated seismicity within 15 km of the Sumatran fault segment in the rupture regions immediately after the 2004, 2005, 2007, and 2010 events, and the seismicity continue to be accumulating during the postseismic relaxation time period. A good correlation between seismicity and stress increase (Fig. 5) suggests that the corresponding Sumatran fault has been stressed since 2004. The stress feedback from the transient postseismic processes is not finished yet, and it will continue loading the Sumatran fault, the surrounding area, and the upper mantle in the years or decades to come (Wang et al., 2012). These transient motions occur quietly on the thrust and its surrounding rocks of the lithosphere and asthenosphere, and are only detectable geodetically (e.g., by GPS). Additionally the area of the Sumatran fault contains many active volcanoes. Our pressure changes estimations warn the possibility of the interaction between them as the secondary effect. Decades of measurements and modeling show that the postseismic relaxation is ongoing (Copley, 2014; Qiu et al., 2018; Suito and Freymueller, 2009), and we need to continue updating the stress maps as well as our hazard assessments.

5. Conclusion

We have developed Coulomb stress models for the Sumatran subduction tectonic region. Specifically, we have evaluated the stress changes in the subduction zone, on the Sumatran fault and at 13 active volcanoes on the Sumatran mainland. We have found that the great earthquake ruptures since 2004 have modified the stress levels over the entire subduction tectonic region. The Mentawai seismic gap and the Sumatran fault have been loaded, posing substantial seismic and tsunami hazards to the neighboring regions. This heightened risk needs to be taken into account by policy makers and to be reflected in hazard assessments.

Declaration of Competing Interest

The authors declared that there is no conflict of interest.

Acknowledgements

This research is supported by the National Research Foundation Singapore and the Singapore Ministry of Education under the Research Centres of Excellence initiative.

Appendix A. Supplementary material

Supplementary data to this article can be found online at https://doi.org/10.1016/j.jseaes.2019.103869.

References

Ammon, C.J., Ji, C., Thio, H.K., Robinson, D., Ni, S., Hjorleifsdottir, V., Kanamori, H., Lay, T., Das, S., Helmberger, D., Ichinose, G., Polet, J., Wald, D., 2005. Rupture process of the 2004 Sumatra-Andaman earthquake. Science 80. https://doi.org/10.1126/science.1112260.

Banerjee, P., Pollitz, F., Nagarajan, B., Bürgmann, R., 2007. Coseismic slip distributions of the 26 December 2004 Sumatra-Andaman and 28 March 2005 Nias earthquakes from GPS static offsets. Bull. Seismol. Soc. Am. 97, 86–102. https://doi.org/10.1785/0120050609.

Barbot, S., Fialko, Y., Bock, Y., 2009. Postseismic deformation due to the Mw 6.0 2004 Parkfield earthquake: Stress-driven creep on a fault with spatially variable rate-and-state friction parameters. J. Geophys. Res. Solid Earth 114. https://doi.org/10.1029/2008JB005748.

Barbot, S., Moore, J.D.P., Lambert, V., 2017. Displacement and stress associated with distributed anelastic deformation in a half-space. Bull. Seismol. Soc. Am. 107, 821–855. https://doi.org/10.1785/0120160237.

Borrero, J.C., Sieh, K., Chlieh, M., Synolakis, C.E., 2006. Tsunami inundation modeling for western Sumatra. Proc. Natl. Acad. Sci. U. S. A. 103, 19673–19677. https://doi.org/10.1073/pnas.0604069103.

Broerse, T., Riva, R., Simons, W., Govers, R., Vermeersen, B., 2015. Postseismic GRACE and GPS observations indicate a rheology contrast above and below the Sumatra slab. J. Geophys. Res. Solid Earth 120, 5343–5361. https://doi.org/10.1002/2015JB011951.

Bürgmann, R., Ergintav, S., Segall, P., Hearn, E.H., McClusky, S., Reilinger, R.E., Woith, H., Zschau, J., 2002. Time-dependent distributed afterslip on and deep below the İzmit earthquake rupture. Bull. Seismol. Soc. Am. 91, 126–137. https://doi.org/10.1785/0120000833.

Catalli, F., Chan, C.H., 2012. New insights into the application of the Coulomb model in real-time. Geophys. J. Int. 188, 583–599. https://doi.org/10.1111/j.1365-246X.2011.05276.x.

Chan, C.H., Sørensen, M.B., Stromeyer, D., Grünthal, G., Heidbach, O., Hakimhashemi, A., Catalli, F., 2010. Forecasting italian seismicity through a spatio-temporal physical model: Importance of considering time-dependency and reliability of the forecast. Ann. Geophys. 53, 129–140. https://doi.org/10.1002/cber.19931260605.

Chan, C.H., Stein, R.S., 2009. Stress evolution following the 1999 Chi-Chi, Taiwan, earthquake: Consequences for afterslip, relaxation, aftershocks and departures from Omori decay. Geophys. J. Int. 177, 179–192. https://doi.org/10.1111/j.1365-246X.2008.04069.x.

Chlieh, M., Avouac, J.P., Hjorleifsdottir, V., Song, T.R.A., Ji, C., Sieh, K., Sladen, A., Hebert, H., Prawirodirdjo, L., Bock, Y., Galetzka, J., 2007. Coseismic slip and afterslip of the great Mw 9.15 Sumatra-Andaman earthquake of 2004. Bull. Seismol. Soc. Am. 97, S152–S173. https://doi.org/10.1785/0120050631.

Chlieh, M., Avouac, J.P., Sieh, K., Natawidjaja, D.H., Galetzka, J., 2008. Heterogeneous coupling of the Sumatran megathrust constrained by geodetic and paleogeodetic measurements. J. Geophys. Res. Solid Earth 113. https://doi.org/10.1029/2007JB004981.

Copley, A., 2014. Postseismic afterslip 30 years after the 1978 Tabas-e-Golshan (Iran) earthquake: observations and implications for the geological evolution of thrust belts. Geophys. J. Int. 179, 665–679. https://doi.org/10.1093/gji/ggu023.

Dieterich, J.H., 1992. Earthquake nucleation on faults with rate-and state-dependent strength. Tectonophysics 211, 115–134. https://doi.org/10.1016/0040-1951(92)90055-B.

Duan, B., Oglesby, D.D., 2006. Heterogeneous fault stresses from previous earthquakes and the effect on dynamics of Parallel strike-slip faults. J. Geophys. Res. Solid Earth 111. https://doi.org/10.1029/2005JB004138.

Felzer, K.R., Becker, T.W., Abercrombie, R.E., Ekström, G., Rice, J.R., 2002. Triggering of the 1999 MW 7.1 Hector Mine earthquake by aftershocks of the 1992 MW 7.3 Landers earthquake. J. Geophys. Res. Solid Earth 107https://doi.org/10.1029/2001JB000911. ESE 6-1–ESE 6-13.

Feng, L., Barbot, S., Hill, E.M., Hermawan, I., Banerjee, P., Natawidjaja, D.H., 2016. Footprints of past earthquakes revealed in the afterslip of the 2010 Mw 7.8 Mentawai tsunami earthquake. Geophys. Res. Lett. 43, 9518–9526. https://doi.org/10.1002/2016GL069870.

Feng, L., Hill, E.M., Banerjee, P., Hermawan, I., Tsang, L.L.H., Natawidjaja, D.H., Suwargadi, B.W., Sieh, K., 2015. A unified GPS-based earthquake catalog for the Sumatran plate boundary between 2002 and 2013. J. Geophys. Res. Solid Earth 120, 3566–3598. https://doi.org/10.1002/2014JB011661.

Freed, A.M., Bürgmann, R., Calais, E., Freymueller, J., Hreinsdóttir, S., 2006. Implications of deformation following the 2002 Denali, Alaska, earthquake for postseismic relaxation processes and lithospheric rheology. J. Geophys. Res. Solid Earth 111. https://doi.org/10.1029/2005JB003894.

Freed, A.M., Lin, J., 2001. Delayed triggering of the 1999 Hector Mine earthquake by viscoelastic stress transfer. Nature 411, 180–183.

Harris, R.A., 1998. Introduction to special section: stress triggers, stress shadows, and implications for seismic hazard. J. Geophys. Res. Solid Earth 103, 24347–24358. https://doi.org/10.1029/98JB01576.

Hearn, E.H., Bürgmann, R., Reilinger, R.E., 2002. Dynamics of İzmit earthquake post-seismic deformation and loading of the Düzce earthquake hypocenter. Bull. Seismol. Soc. Am. 92, 172–193. https://doi.org/10.1785/0120000832.

Hill, E.M., Borrero, J.C., Huang, Z., Qiu, Q., Banerjee, P., Natawidjaja, D.H., Elosegui, P., Fritz, H.M., Suwargadi, B.W., Pranantyo, I.R., Li, L., Macpherson, K.A., Skanavis, V., Synolakis, C.E., Sieh, K., 2012. The 2010 M w 7.8 Mentawai earthquake: Very shallow source of a rare tsunami earthquake determined from tsunami field survey and near-field GPS data. J. Geophys. Res. 117, B06402. https://doi.org/10.1029/2012JB009159.

Hill, E.M., Yue, H., Barbot, S., Lay, T., Tapponnier, P., Hermawan, I., Hubbard, J., Banerjee, P., Feng, L., Natawidjaja, D., Sieh, K., 2015. The 2012 Mw8.6 Wharton Basin sequence: A cascade of great earthquakes generated by near-orthogonal, young, oceanic mantle faults. J. Geophys. Res. Solid Earth 120, 3723–3747. https://doi.org/10.1111/mec.13688.

Hoechner, A., Sobolev, S.V., Einarsson, I., Wang, R., 2011. Investigation on afterslip and steady state and transient rheology based on postseismic deformation and geoid change caused by the Sumatra 2004 earthquake. Geochem., Geophys. Geosyst. 12, Q07010. https://doi.org/10.1029/2010GC003450.

Hsu, Y.-J., Bechor, N., Segall, P., Yu, S.-B., Kuo, L.-C., Ma, K.-F., 2002. Rapid afterslip following the 1999 Chi-Chi, Taiwan Earthquake. Geophys. Res. Lett. 29https://doi.org/10.1029/2002GL014967. 1-4-1–4.

Hu, Y., Bürgmann, R., Banerjee, P., Feng, L., Hill, E.M., Ito, T., Tabei, T., Wang, K., 2016. Asthenosphere rheology inferred from observations of the 2012 Indian Ocean earthquake. Nature 538, 368–372. https://doi.org/10.1038/nature19787.

Hu, Y., Wang, K., 2012. Spherical-Earth finite element model of short-term postseismic deformation following the 2004 Sumatra earthquake. J. Geophys. Res. Solid Earth 117, B05404. https://doi.org/10.1029/2012JB009153.

Hughes, K.L.H., Masterlark, T., Mooney, W.D., 2010. Poroelastic stress-triggering of the 2005 M8.7 Nias earthquake by the 2004 M9.2 Sumatra-Andaman earthquake. Earth Planet. Sci. Lett. 293, 289–299. https://doi.org/10.1016/j.epsl.2010.02.043.

Johnson, K.M., Bürgmann, R., Larson, K., 2006. Frictional Properties on the San Andreas Fault near Parkfield, California, Inferred from Models of Afterslip following the 2004 Earthquake. Bull. Seismol. Soc. Am. 96, S321–S338.

King, G.C.P., Cocco, M., 2001. Fault interaction by elastic stress changes: New clues from earthquake sequences. Adv. Geophys. 44https://doi.org/10.1016/S0065-2687(00)80006-0. 1–VIII.

Klein, E., Fleitout, L., Vigny, C., Garaud, J.D., 2016. Afterslip and viscoelastic relaxation model inferred from the large-scale post-seismic deformation following the 2010 Mw8.8 Maule earthquake (Chile). Geophys. J. Int. 205, 1455–1472. https://doi.org/10.1093/gji/ggw086.

Konca, A.O., Hjorleifsdottir, V., Song, T.-R.A., Avouac, J.-P., Helmberger, D.V., Ji, C., Sieh, K., Briggs, R., Meltzner, A., 2007. Rupture kinematics of the 2005 Mw 8.6 Nias-simeulue earthquake from the joint inversion of seismic and geodetic data. Bull. Seismol. Soc. Am. 97, S307–S322. https://doi.org/10.1785/0120050632.

Konca, A.O., Avouac, J.-P., Sladen, A., Meltzner, A.J., Sieh, K., Fang, P., Li, Z., Galetzka, J., Genrich, J., Chlieh, M., Natawidjaja, D.H., Bock, Y., Fielding, E.J., Ji, C., Helmberger, D.V., 2008. Partial rupture of a locked patch of the Sumatra megathrust during the 2007 earthquake sequence. Nature 456, 631–635.

Kreemer, C., Blewitt, G., Maerten, F., 2006. Co- and postseismic deformation of the 28 March 2005 Nias Mw 8.7 earthquake from continuous GPS data. Geophys. Res. Lett. 33. https://doi.org/10.1029/2005GL025566.

Lapusta, N., Rice, J.R., 2003. Nucleation and early seismic propagation of small and large events in a crustal earthquake model. J. Geophys. Res. Solid Earth 108. https://doi.org/10.1029/2001JB000793.

Li, L., Huang, Z., Qiu, Q., Natawidjaja, D.H., Sieh, K., 2012. Tsunami-induced coastal change: scenario studies for Painan, West Sumatra, Indonesia. Earth, Planets Sp. 64, 2. https://doi.org/10.5047/eps.2011.08.002.

Li, S., Bedford, J., Moreno, M., Barnhart, W.D., Rosenau, M., Oncken, O., 2018. Spatiotemporal Variation of Mantle Viscosity and the Presence of Cratonic Mantle Inferred From 8 Years of Postseismic Deformation Following the 2010 Maule, Chile, Earthquake. Geochem., Geophys. Geosyst. 3272–3285. https://doi.org/10.1029/2018GC007645.

Linette, P., Robert, M., David, C.C., Yehuda, B., Cecep, S., 2010. Geodetic observations of an earthquake cycle at the Sumatra subduction zone: Role of interseismic strain segmentation. J. Geophys. Res. Solid Earth 115. https://doi.org/10.1029/2008JB006139.

Masuti, S., Barbot, S.D., Karato, S., Feng, L., Banerjee, P., 2016. Upper-mantle water stratification inferred from observations of the 2012 Indian Ocean earthquake. Nature 538, 373–377.

Moore, J.D.P., Yu, H., Tang, C.-H., Wang, T., Barbot, S., Peng, D., Masuti, S., Dauwels, J., Hsu, Y.-J., Lambert, V., Nanjundiah, P., Wei, S., Lindsey, E., Feng, L., Shibazaki, B., 2017. Imaging the distribution of transient viscosity after the 2016 Mw 7.1 Kumamoto earthquake. Science 80 (356), 163–167. https://doi.org/10.1126/science.aal3422.

Muhari, A., Imamura, F., Natawidjaja, D.H., Diposaptono, S., Latief, H., Post, J., Ismail, F.A., 2010. Tsunami mitigation efforts with pTA in west Sumatra province, Indonesia. J. Earthq. Tsunami 04, 341–368. https://doi.org/10.1142/S1793431110000790.

Natawidjaja, D., 2009. Scenario for future megathrust tsunami event in the Sumatran subduction zone. In: Proceedings of the Asian Oceania Geo-Sciences Society (AOGS) Meeting, Singapore, 2009.

Natawidjaja, D.H., Sieh, K., Chlieh, M., Galetzka, J., Suwargadi, B.W., Cheng, H., Edwards, R.L., Avouac, J.P., Ward, S.N., 2006. Source parameters of the great Sumatran megathrust earthquakes of 1797 and 1833 inferred from coral microatolls. J. Geophys. Res. Solid Earth 111. https://doi.org/10.1029/2005JB004025.

Natawidjaja, D.H., Sieh, K., Galetzka, J., Suwargadi, B.W., Cheng, H., Edwards, R.L., Chlieh, M., 2007. Interseismic deformation above the Sunda Megathrust recorded in coral microatolls of the Mentawai islands, West Sumatra. J. Geophys. Res. Solid Earth 112. https://doi.org/10.1029/2006JB004450.

Panet, I., Pollitz, F., Mikhailov, V., Diament, M., Banerjee, P., Grijalva, K., 2010. Upper mantle rheology from GRACE and GPS postseismic deformation after the 2004 Sumatra-Andaman earthquake. Geochem., Geophys. Geosyst. 11, Q06008. https://doi.org/10.1029/2009GC002905.

Perfettini, H., Avouac, J.-P., 2007. Modeling afterslip and aftershocks following the 1992 Landers earthquake. J. Geophys. Res. Solid Earth 112. https://doi.org/10.1029/2006JB004399.

Pollitz, F.F., Bürgmann, R., Banerjee, P., 2006. Post-seismic relaxation following the great 2004 Sumatra-Andaman earthquake on a compressible self-gravitating Earth. Geophys. J. Int. 167, 397–420. https://doi.org/10.1111/j.1365-246X.2006.03018.x.

Pritchard, M.E., Jay, J.A., Aron, F., Henderson, S.T., Lara, L.E., 2013. Subsidence at southern Andes volcanoes induced by the 2010 Maule. Chile Earthq.. Nat. Geosci. 6, 632. https://doi.org/10.1038/ngeo1855.

Qiu, Q.D.P., Moore, J., Barbot, S., Feng, L., Hill, E.M., 2018. Transient rheology of the Sumatran mantle wedge revealed by a decade of great earthquakes. Nat. Commun. 9. https://doi.org/10.1038/s41467-018-03298-6.

Salman, R., Hill, E.M., Feng, L., Lindsey, E.O., Mele veedu, D., Barbot, S., Banerjee, P., Hermawan, I., Natawidjaja, D.H., 2017. Piecemeal rupture of the Mentawai Patch, Sumatra: The 2008 Mw7.2 North Pagai earthquake sequence. J. Geophys. Res. Solid Earth 1–16. https://doi.org/10.1002/2017JB014341.

Sieh, K., Natawidjaja, D., 2000. Neotectonics of the Sumatran fault, Indonesia. J. Geophys. Res. Solid Earth 105, 28295–28326. https://doi.org/10.1029/2000JB900120.

Sieh, K., Natawidjaja, D.H., Meltzner, A.J., Shen, C.C., Cheng, H., Li, K.S., Suwargadi, B.W., Galetzka, J., Philibosian, B., Edwards, R.L., 2008. Earthquake supercycles inferred from sea-level changes recorded in the corals of west Sumatra. Science 80 (322), 1674–1678. https://doi.org/10.1126/science.1163589.

Sladen, A., Trevisan, J., 2018. Shallow megathrust earthquake ruptures betrayed by their outer-trench aftershocks signature. Earth Planet. Sci. Lett. 483, 105–113. https://doi.org/10.1016/j.epsl.2017.12.006.

Suito, H., Freymueller, J.T., 2009. A viscoelastic and afterslip postseismic deformation model for the 1964 Alaska earthquake. J. Geophys. Res. Solid Earth 114. https://doi.org/10.1029/2008JB005954.

Sun, T., Wang, K., Iinuma, T., Hino, R., He, J., Fujimoto, H., Kido, M., Osada, Y., Miura, S., Ohta, Y., Hu, Y., 2014. Prevalence of viscoelastic relaxation after the 2011 Tohoku-oki earthquake. Nature 514, 84–87.

Toda, S., Lin, J., Meghraoui, M., Stein, R.S., 2008. 12 May 2008 M = 7.9 Wenchuan, China, earthquake calculated to increase failure stress and seismicity rate on three major fault systems. Geophys. Res. Lett. 35. https://doi.org/10.1029/2008GL034903.

Toda, S., Stein, R.S., Sevilgen, V., Lin, J., 2011. Coulomb 3.3 Graphic-rich deformation and stress-change software for earthquake, tectonic, and volcano research and teaching—user guide:Rep. Earthquake Science Center, Menlo Park Science Center, Menlo Park, California 63 pp.

Tsang, L.L.H., Hill, E.M., Barbot, S., Qiu, Q., Feng, L., Hermawan, I., Banerjee, P., Natawidjaja, D.H., 2016. Afterslip following the 2007 Mw 8.4 Bengkulu earthquake in Sumatra loaded the 2010 Mw 7.8 Mentawai tsunami earthquake rupture zone. J. Geophys. Res. Solid Earth 121, 9034–9049. https://doi.org/10.1002/2016JB013432.

Wang, K., Hu, Y., He, J., 2012. Deformation cycles of subduction earthquakes in a viscoelastic Earth. Nature 484, 327. https://doi.org/10.1038/nature11032.

Wiseman, K., Bürgmann, R., Freed, A.M., Banerjee, P., 2015. Viscoelastic relaxation in a heterogeneous Earth following the 2004 Sumatra-Andaman earthquake. Earth Planet. Sci. Lett. 431, 308–317. https://doi.org/https://doi.org/10.1016/j.epsl.2015.09.024.